Figure S1

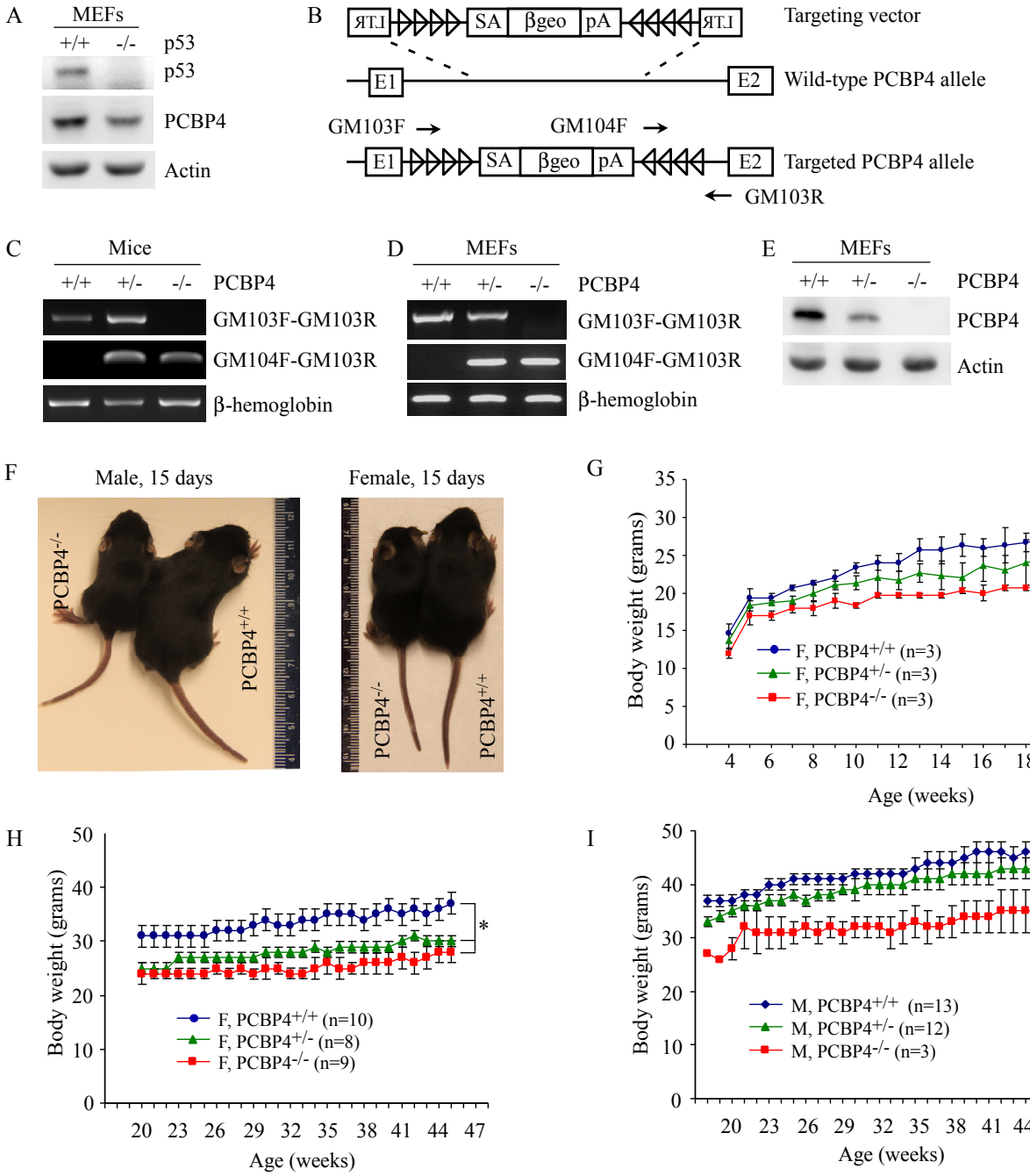

Figure S1. Generation of *PCBP4* knockout mice and MEFs. *(A)* The level of PCBP4 protein was measured in WT and *p53*$^{-/-}$ MEFs. *(B) PCBP4* knockout strategy and primers used for genotyping. The *PCBP4* gene was disrupted by insertion of a gene trap (rFRosaβgeo+1s) into the first intron. Primers GM103F and GM103R were used for genotyping wild-type *PCBP4* allele; primers GM104F and GM103R were used for genotyping the null allele. *(C)* Genotyping of WT, *PCBP4*$^{+/-}$, and *PCBP4*$^{-/-}$ mice. Top and middle panels represent wild-type and knockout alleles of *PCBP4*, respectively. Bottom panel: β-hemoglobin was measured as an internal control. *(D)* Genotyping of *PCBP4* knockout MEFs. *(E)* The level of PCBP4 protein was measured in WT, *PCBP4*$^{+/-}$, and *PCBP4*$^{-/-}$ MEFs. Actin was measured as an internal control. *(F)* Representative images of 15-day-old WT and *PCBP4*$^{-/-}$ male and female littermates. *(G)* The body weight of *WT*, *PCBP4*$^{+/-}$, and *PCBP4*$^{-/-}$ female mice was measured each week from 4-19 weeks of age. Data are presented as means ± SDs. * $P<0.05$. (H) The body weight of WT, *PCBP4*$^{+/-}$, and *PCBP4*$^{-/-}$ female mice was measured each week from 20-45 weeks of age. *(I)* The body weight of WT, *PCBP4*$^{+/-}$, and *PCBP4*$^{-/-}$ male mice was measured each week from 18-45 weeks of age.

Figure S2

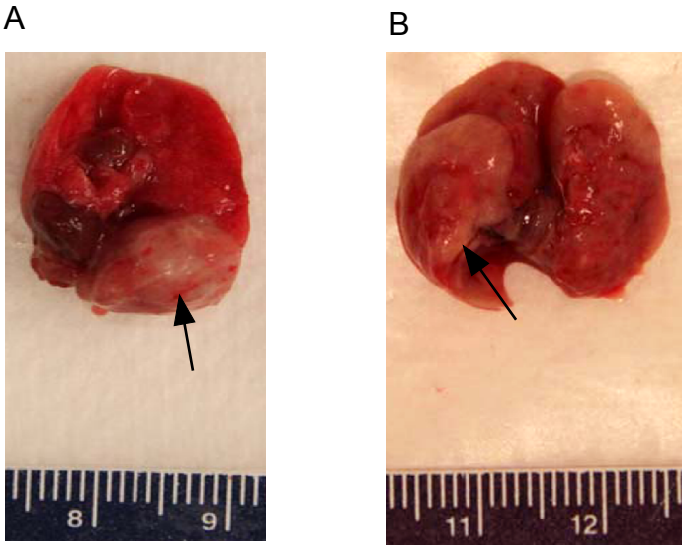

PCBP4$^{-/-}$ lung tissue PCBP4$^{-/-}$ lung tissue

Figure S2. ***PCBP4*** **knockout mice are prone to lung cancer**. *(A-B)* Representative images of lung tissues from two *PCBP4*$^{-/-}$ mice. The main tick mark of the ruler represents one centimeter.

Figure S3

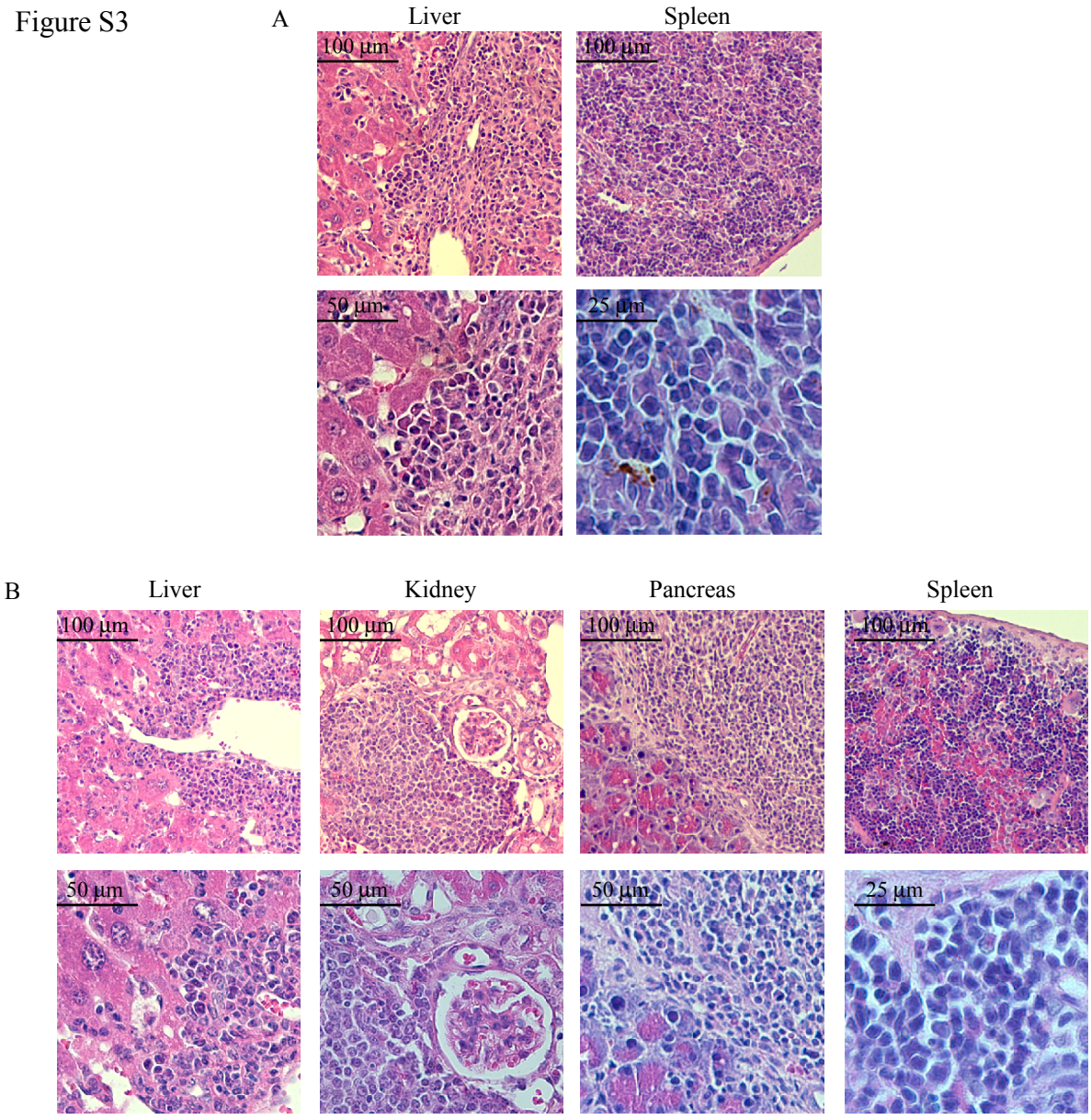

Figure S3. *PCBP4* knockout mice are prone to lymphoma. *(A)* Representative images of HE-stained sections of liver and spleen from *PCBP4*$^{+/-}$ mice. *(B)* Representative images of HE-stained sections of liver, kidney, pancreas, and spleen from *PCBP4*$^{-/-}$ mice.

Figure S4

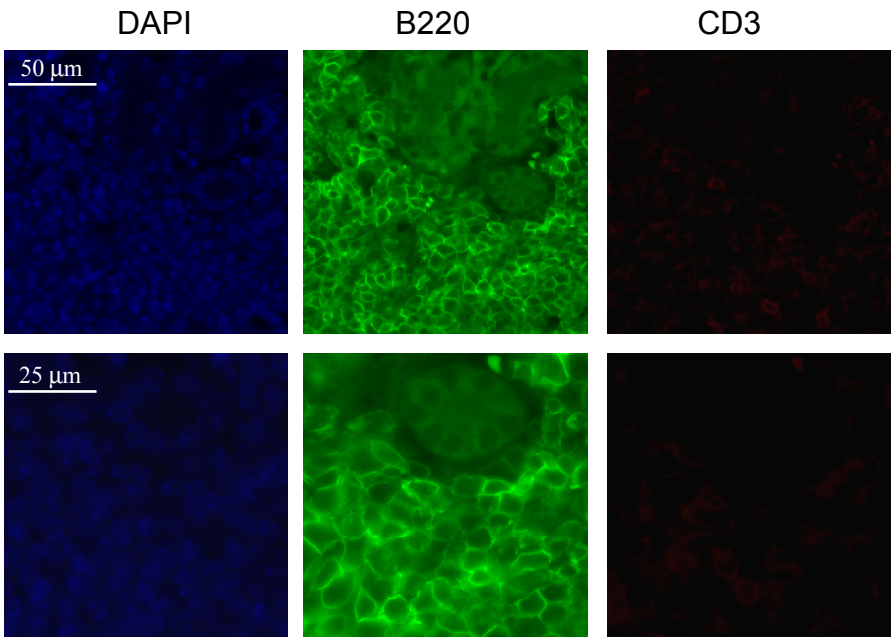

Figure S4. ***PCBP4*** **knockout mice are prone to B-cell lymphoma**. Representative images of immunofluorescence-stained kidney sections of *PCBP4*$^{-/-}$ mice with antibodies against B-cell marker B220 and T-cell marker CD3, respectively.

Figure S5

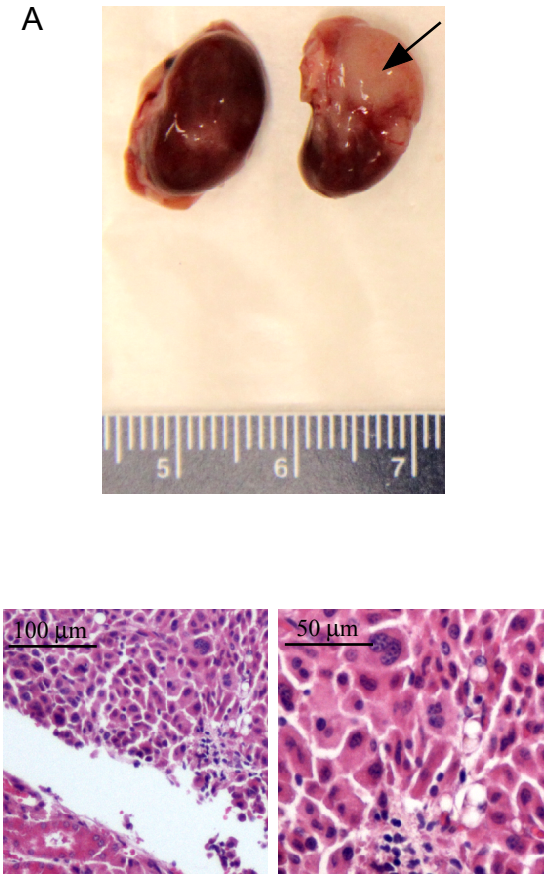

Figure S5. Kidney tumors in *PCBP*4-deficient mice. *(A)* Representative image of kidney tumor in one *PCBP4*$^{-/-}$ mouse. The main tick mark of the ruler represents one centimeter. *(B)* Representative images of HE-stained kidney tumor in one *PCBP4*$^{+/-}$ mouse.

Figure S6

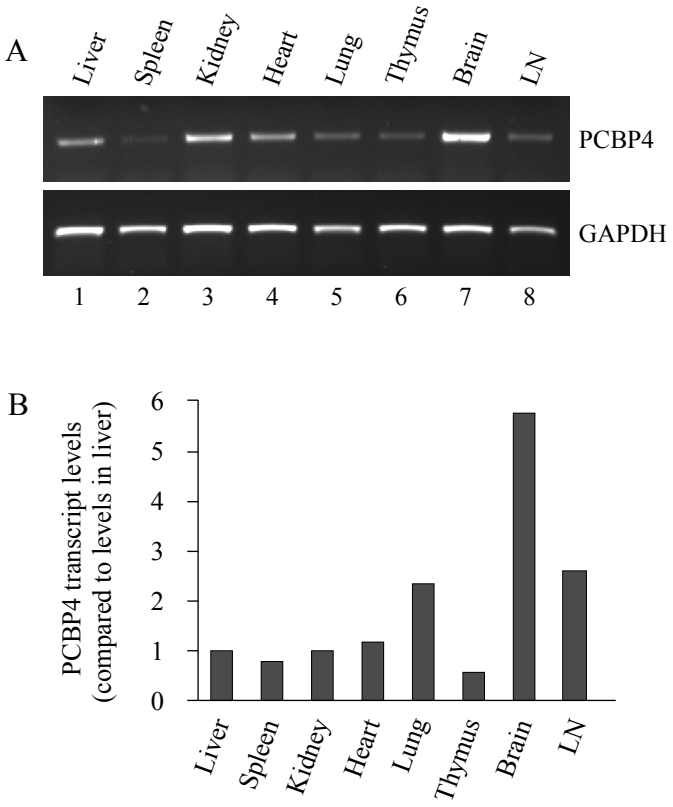

Figure S6. The level of PCBP4 transcript in eight tissues of wild-type mouse. *(A)* RT-PCR was performed to measure the levels of PCBP4 transcript in mouse liver, spleen, kidney, heart, lung, thymus, brain, and lymph node (LN). GAPDH was measured and used as a loading control. *(B)* The relative levels of PCBP4 transcript measured in (A) were normalized by level of GAPDH and then compared to the level of PCBP4 in liver.

Figure S7

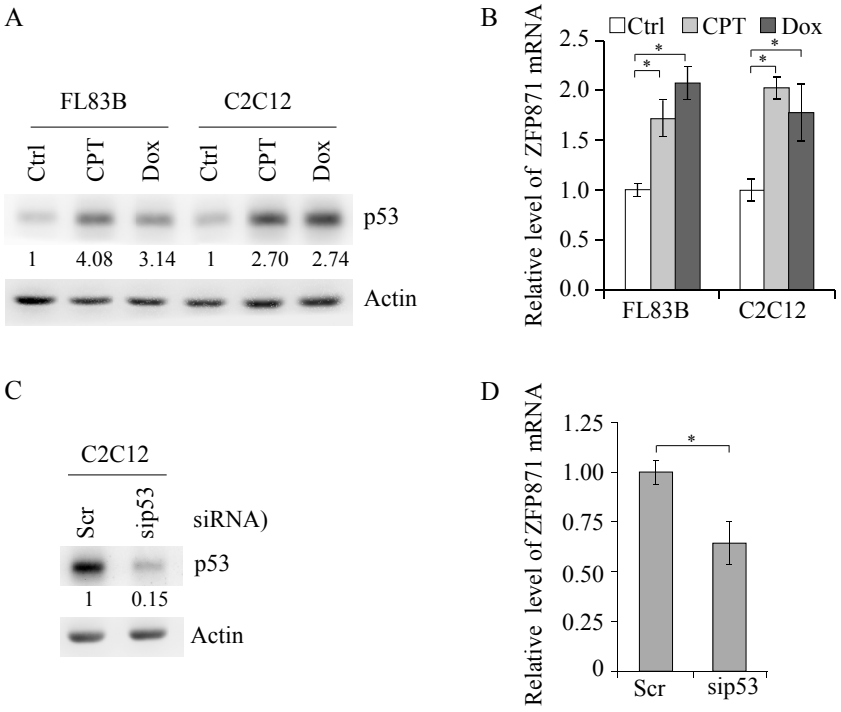

Figure S7. The expression of ZFP871 is increased by activation of p53 but decreased by knockdown of p53 in cells. *(A)* The levels of p53 and actin proteins were measured in FL83B and C2C12 cells, untreated or treated with 300 nM camptothecin or 0.3 μg/ml doxorubicin for 24 h. *(B)* The level of ZFP871 mRNA was measured by qRT-PCR in FL83B and C2C12 cells, treated as in *(A)*. Data were presented as means ± SDs normalized to actin mRNA from three separate experiments. **P*<0.05. *(C)* The levels of p53 and actin proteins were measured in C2C12 cells transfected with scrambled siRNA or siRNA against p53 for 3 day. *(D)* The level of ZFP871 mRNA was measured by qRT-PCR in C2C12 cells, treated as in *(C)*. Data were presented as means ± SDs normalized to actin mRNA from three separate experiments. **P*<0.05.

Figure S8

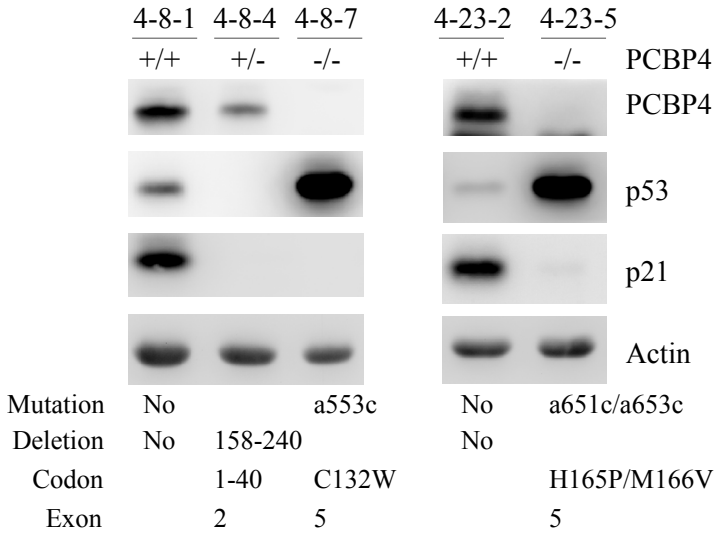

Figure S8. The *p53* gene is prone to mutation in immortalized *PCBP4*-deficient MEFs. The levels of PCBP4, p53, and p21 proteins were measured in two sets of immortalized WT, *PCBP4*$^{+/-}$ and *PCBP4*$^{-/-}$ littermate MEFs. Actin was used as a loading control. The mutation or deletion of the *p53* gene was determined by sequencing p53 cDNA from each line of MEFs and listed below the western blots.

Figure S9

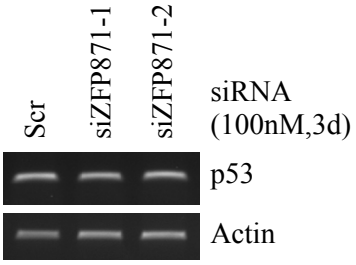

Figure S9. The level of p53 transcript was measured in C2C12 cells transfected with a scrambled siRNA or one of the two unique siRNAs against ZFP871. Actin was measured and used as a loading control.

Figure S10

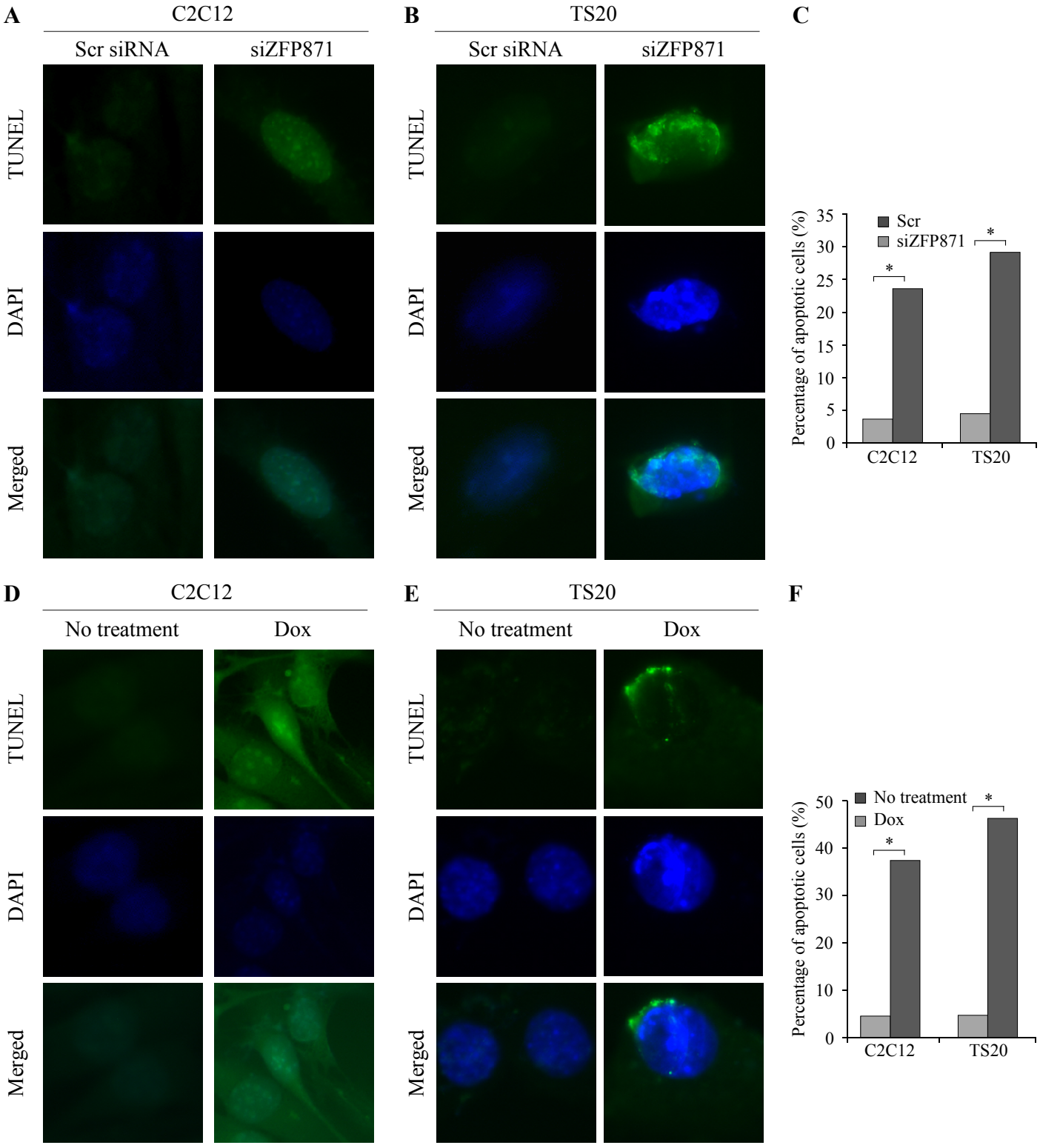

Figure S10. Knockdown of ZFP871 and treatment with doxorubicin lead to apoptosis in C2C12 and TS20 cells. *(A-B)* The apoptotic cells were measured with TUNEL assay in C2C12 *(A)* and TS20 *(B)* cells transfected with scrambled siRNA or siRNA against ZFP871 for 3 d. *(C)* The percentage of apoptotic cells shown in *(A-B)*. *$P<0.05$. *(D-E)* The apoptotic cells were measured with TUNEL assay in C2C12 *(D)* and TS20*(D)* cells untreated or treated with 0.3 μg/ml doxorubicin for 24 h. *(F)* The percentage of apoptotic cells shown in *(D-E)*. *$P<0.05$.